Measurement of the b Jet Cross Section in Events with a Z Boson in $p\overline{p}$ Collisions at $\sqrt{s}$=1.96 TeV

A. Abulencia,[23] D. Acosta,[17] J. Adelman,[13] T. Affolder,[10] T. Akimoto,[55] M.G. Albrow,[16] D. Ambrose,[16] S. Amerio,[43] D. Amidei,[34] A. Anastassov,[52] K. Anikeev,[16] A. Annovi,[18] J. Antos,[1] M. Aoki,[55] G. Apollinari,[16] J.-F. Arguin,[33] T. Arisawa,[57] A. Artikov,[14] W. Ashmanskas,[16] A. Attal,[8] F. Azfar,[42] P. Azzi-Bacchetta,[43] P. Azzurri,[46] N. Bacchetta,[43] H. Bachacou,[28] W. Badgett,[16] A. Barbaro-Galtieri,[28] V.E. Barnes,[48] B.A. Barnett,[24] S. Baroiant,[7] V. Bartsch,[30] G. Bauer,[32] F. Bedeschi,[46] S. Behari,[24] S. Belforte,[54] G. Bellettini,[46] J. Bellinger,[59] A. Belloni,[32] E. Ben Haim,[44] D. Benjamin,[15] A. Beretvas,[16] J. Beringer,[28] T. Berry,[29] A. Bhatti,[50] M. Binkley,[16] D. Bisello,[43] R. E. Blair,[2] C. Blocker,[6] B. Blumenfeld,[24] A. Bocci,[15] A. Bodek,[49] V. Boisvert,[49] G. Bolla,[48] A. Bolshov,[32] D. Bortoletto,[48] J. Boudreau,[47] A. Boveia,[10] B. Brau,[10] C. Bromberg,[35] E. Brubaker,[13] J. Budagov,[14] H.S. Budd,[49] S. Budd,[23] K. Burkett,[16] G. Busetto,[43] P. Bussey,[20] K. L. Byrum,[2] S. Cabrera,[15] M. Campanelli,[19] M. Campbell,[34] F. Canelli,[8] A. Canepa,[48] D. Carlsmith,[59] R. Carosi,[46] S. Carron,[15] M. Casarsa,[54] A. Castro,[5] P. Catastini,[46] D. Cauz,[54] M. Cavalli-Sforza,[3] A. Cerri,[28] L. Cerrito,[42] S.H. Chang,[27] J. Chapman,[34] Y.C. Chen,[1] M. Chertok,[7] G. Chiarelli,[46] G. Chlachidze,[14] F. Chlebana,[16] I. Cho,[27] K. Cho,[27] D. Chokheli,[14] J.P. Chou,[21] P.H. Chu,[23] S.H. Chuang,[59] K. Chung,[12] W.H. Chung,[59] Y.S. Chung,[49] M. Ciljak,[46] C.I. Ciobanu,[23] M.A. Ciocci,[46] A. Clark,[19] D. Clark,[6] M. Coca,[15] G. Compostella,[43] M.E. Convery,[50] J. Conway,[7] B. Cooper,[30] K. Copic,[34] M. Cordelli,[18] G. Cortiana,[43] F. Cresciolo,[46] A. Cruz,[17] C. Cuenca Almenar,[7] J. Cuevas,[11] R. Culbertson,[16] D. Cyr,[59] S. DaRonco,[43] S. D'Auria,[20] M. D'Onofrio,[3] D. Dagenhart,[6] P. de Barbaro,[49] S. De Cecco,[51] A. Deisher,[28] G. De Lentdecker,[49] M. Dell'Orso,[46] F. Delli Paoli,[43] S. Demers,[49] L. Demortier,[50] J. Deng,[15] M. Deninno,[5] D. De Pedis,[51] P.F. Derwent,[16] C. Dionisi,[51] J.R. Dittmann,[4] P. DiTuro,[52] C. Dörr,[25] S. Donati,[46] M. Donega,[19] P. Dong,[8] J. Donini,[43] T. Dorigo,[43] S. Dube,[52] K. Ebina,[57] J. Efron,[39] J. Ehlers,[19] R. Erbacher,[7] D. Errede,[23] S. Errede,[23] R. Eusebi,[16] H.C. Fang,[28] S. Farrington,[29] I. Fedorko,[46] W.T. Fedorko,[13] R.G. Feild,[60] M. Feindt,[25] J.P. Fernandez,[31] R. Field,[17] G. Flanagan,[48] L.R. Flores-Castillo,[47] A. Foland,[21] S. Forrester,[7] G.W. Foster,[16] M. Franklin,[21] J.C. Freeman,[28] I. Furic,[13] M. Gallinaro,[50] J. Galyardt,[12] J.E. Garcia,[46]

M. Garcia Sciveres,[28] A.F. Garfinkel,[48] C. Gay,[60] H. Gerberich,[23] D. Gerdes,[34] S. Giagu,[51] P. Giannetti,[46] A. Gibson,[28] K. Gibson,[12] C. Ginsburg,[16] N. Giokaris,[14] K. Giolo,[48] M. Giordani,[54] P. Giromini,[18] M. Giunta,[46] G. Giurgiu,[12] V. Glagolev,[14] D. Glenzinski,[16] M. Gold,[37] N. Goldschmidt,[34] J. Goldstein,[42] G. Gomez,[11] G. Gomez-Ceballos,[11] M. Goncharov,[53] O. González,[31] I. Gorelov,[37] A.T. Goshaw,[15] Y. Gotra,[47] K. Goulianos,[50] A. Gresele,[43] M. Griffiths,[29] S. Grinstein,[21] C. Grosso-Pilcher,[13] R.C. Group,[17] U. Grundler,[23] J. Guimaraes da Costa,[21] Z. Gunay-Unalan,[35] C. Haber,[28] S.R. Hahn,[16] K. Hahn,[45] E. Halkiadakis,[52] A. Hamilton,[33] B.-Y. Han,[49] J.Y. Han,[49] R. Handler,[59] F. Happacher,[18] K. Hara,[55] M. Hare,[56] S. Harper,[42] R.F. Harr,[58] R.M. Harris,[16] K. Hatakeyama,[50] J. Hauser,[8] C. Hays,[15] A. Heijboer,[45] B. Heinemann,[29] J. Heinrich,[45] M. Herndon,[59] D. Hidas,[15] C.S. Hill,[10] D. Hirschbuehl,[25] A. Hocker,[16] A. Holloway,[21] S. Hou,[1] M. Houlden,[29] S.-C. Hsu,[9] B.T. Huffman,[42] R.E. Hughes,[39] J. Huston,[35] J. Incandela,[10] G. Introzzi,[46] M. Iori,[51] Y. Ishizawa,[55] A. Ivanov,[7] B. Iyutin,[32] E. James,[16] D. Jang,[52] B. Jayatilaka,[34] D. Jeans,[51] H. Jensen,[16] E.J. Jeon,[27] S. Jindariani,[17] M. Jones,[48] K.K. Joo,[27] S.Y. Jun,[12] T.R. Junk,[23] T. Kamon,[53] J. Kang,[34] P.E. Karchin,[58] Y. Kato,[41] Y. Kemp,[25] R. Kephart,[16] U. Kerzel,[25] V. Khotilovich,[53] B. Kilminster,[39] D.H. Kim,[27] H.S. Kim,[27] J.E. Kim,[27] M.J. Kim,[12] S.B. Kim,[27] S.H. Kim,[55] Y.K. Kim,[13] L. Kirsch,[6] S. Klimenko,[17] M. Klute,[32] B. Knuteson,[32] B.R. Ko,[15] H. Kobayashi,[55] K. Kondo,[57] D.J. Kong,[27] J. Konigsberg,[17] A. Korytov,[17] A.V. Kotwal,[15] A. Kovalev,[45] A. Kraan,[45] J. Kraus,[23] I. Kravchenko,[32] M. Kreps,[25] J. Kroll,[45] N. Krumnack,[4] M. Kruse,[15] V. Krutelyov,[53] S. E. Kuhlmann,[2] Y. Kusakabe,[57] S. Kwang,[13] A.T. Laasanen,[48] S. Lai,[33] S. Lami,[46] S. Lammel,[16] M. Lancaster,[30] R.L. Lander,[7] K. Lannon,[39] A. Lath,[52] G. Latino,[46] I. Lazzizzera,[43] T. LeCompte,[2] J. Lee,[49] J. Lee,[27] Y.J. Lee,[27] S.W. Lee,[53] R. Lefèvre,[3] N. Leonardo,[32] S. Leone,[46] S. Levy,[13] J.D. Lewis,[16] C. Lin,[60] C.S. Lin,[16] M. Lindgren,[16] E. Lipeles,[9] T.M. Liss,[23] A. Lister,[19] D.O. Litvintsev,[16] T. Liu,[16] N.S. Lockyer,[45] A. Loginov,[36] M. Loreti,[43] P. Loverre,[51] R.-S. Lu,[1] D. Lucchesi,[43] P. Lujan,[28] P. Lukens,[16] G. Lungu,[17] L. Lyons,[42] J. Lys,[28] R. Lysak,[1] E. Lytken,[48] P. Mack,[25] D. MacQueen,[33] R. Madrak,[16] K. Maeshima,[16] T. Maki,[22] P. Maksimovic,[24] S. Malde,[42] G. Manca,[29] F. Margaroli,[5] R. Marginean,[16] C. Marino,[23] A. Martin,[60] V. Martin,[38] M. Martínez,[3] T. Maruyama,[55] H. Matsunaga,[55] M.E. Mattson,[58] R. Mazini,[33]

P. Mazzanti,[5] K.S. McFarland,[49] P. McIntyre,[53] R. McNulty,[29] A. Mehta,[29] S. Menzemer,[11] A. Menzione,[46] P. Merkel,[48] C. Mesropian,[50] A. Messina,[51] M. von der Mey,[8] T. Miao,[16] N. Miladinovic,[6] J. Miles,[32] R. Miller,[35] J.S. Miller,[34] C. Mills,[10] M. Milnik,[25] R. Miquel,[28] A. Mitra,[1] G. Mitselmakher,[17] A. Miyamoto,[26] N. Moggi,[5] B. Mohr,[8] R. Moore,[16] M. Morello,[46] P. Movilla Fernandez,[28] J. Mülmenstädt,[28] A. Mukherjee,[16] Th. Muller,[25] R. Mumford,[24] P. Murat,[16] J. Nachtman,[16] J. Naganoma,[57] S. Nahn,[32] I. Nakano,[40] A. Napier,[56] D. Naumov,[37] V. Necula,[17] C. Neu,[45] M.S. Neubauer,[9] J. Nielsen,[28] T. Nigmanov,[47] L. Nodulman,[2] O. Norniella,[3] E. Nurse,[30] T. Ogawa,[57] S.H. Oh,[15] Y.D. Oh,[27] T. Okusawa,[41] R. Oldeman,[29] R. Orava,[22] K. Osterberg,[22] C. Pagliarone,[46] E. Palencia,[11] R. Paoletti,[46] V. Papadimitriou,[16] A.A. Paramonov,[13] B. Parks,[39] S. Pashapour,[33] J. Patrick,[16] G. Pauletta,[54] M. Paulini,[12] C. Paus,[32] D.E. Pellett,[7] A. Penzo,[54] T.J. Phillips,[15] G. Piacentino,[46] J. Piedra,[44] L. Pinera,[17] K. Pitts,[23] C. Plager,[8] L. Pondrom,[59] X. Portell,[3] O. Poukhov,[14] N. Pounder,[42] F. Prakoshyn,[14] A. Pronko,[16] J. Proudfoot,[2] F. Ptohos,[18] G. Punzi,[46] J. Pursley,[24] J. Rademacker,[42] A. Rahaman,[47] A. Rakitin,[32] S. Rappoccio,[21] F. Ratnikov,[52] B. Reisert,[16] V. Rekovic,[37] N. van Remortel,[22] P. Renton,[42] M. Rescigno,[51] S. Richter,[25] F. Rimondi,[5] L. Ristori,[46] W.J. Robertson,[15] A. Robson,[20] T. Rodrigo,[11] E. Rogers,[23] S. Rolli,[56] R. Roser,[16] M. Rossi,[54] R. Rossin,[17] C. Rott,[48] A. Ruiz,[11] J. Russ,[12] V. Rusu,[13] H. Saarikko,[22] S. Sabik,[33] A. Safonov,[53] W.K. Sakumoto,[49] G. Salamanna,[51] O. Saltó,[3] D. Saltzberg,[8] C. Sanchez,[3] L. Santi,[54] S. Sarkar,[51] L. Sartori,[46] K. Sato,[55] P. Savard,[33] A. Savoy-Navarro,[44] T. Scheidle,[25] P. Schlabach,[16] E.E. Schmidt,[16] M.P. Schmidt,[60] M. Schmitt,[38] T. Schwarz,[34] L. Scodellaro,[11] A.L. Scott,[10] A. Scribano,[46] F. Scuri,[46] A. Sedov,[48] S. Seidel,[37] Y. Seiya,[41] A. Semenov,[14] L. Sexton-Kennedy,[16] I. Sfiligoi,[18] M.D. Shapiro,[28] T. Shears,[29] P.F. Shepard,[47] D. Sherman,[21] M. Shimojima,[55] M. Shochet,[13] Y. Shon,[59] I. Shreyber,[36] A. Sidoti,[44] P. Sinervo,[33] A. Sisakyan,[14] J. Sjolin,[42] A. Skiba,[25] A.J. Slaughter,[16] K. Sliwa,[56] J.R. Smith,[7] F.D. Snider,[16] R. Snihur,[33] M. Soderberg,[34] A. Soha,[7] S. Somalwar,[52] V. Sorin,[35] J. Spalding,[16] M. Spezziga,[16] F. Spinella,[46] T. Spreitzer,[33] P. Squillacioti,[46] M. Stanitzki,[60] A. Staveris-Polykalas,[46] R. St. Denis,[20] B. Stelzer,[8] O. Stelzer-Chilton,[42] D. Stentz,[38] J. Strologas,[37] D. Stuart,[10] J.S. Suh,[27] A. Sukhanov,[17] K. Sumorok,[32] H. Sun,[56] T. Suzuki,[55] A. Taffard,[23] R. Takashima,[40] Y. Takeuchi,[55] K. Takikawa,[55] M. Tanaka,[2]

R. Tanaka,[40] N. Tanimoto,[40] M. Tecchio,[34] P.K. Teng,[1] K. Terashi,[50] S. Tether,[32] J. Thom,[16] A.S. Thompson,[20] E. Thomson,[45] P. Tipton,[49] V. Tiwari,[12] S. Tkaczyk,[16] D. Toback,[53] S. Tokar,[14] K. Tollefson,[35] T. Tomura,[55] D. Tonelli,[46] M. Tönnesmann,[35] S. Torre,[18] D. Torretta,[16] S. Tourneur,[44] W. Trischuk,[33] R. Tsuchiya,[57] S. Tsuno,[40] N. Turini,[46] F. Ukegawa,[55] T. Unverhau,[20] S. Uozumi,[55] D. Usynin,[45] A. Vaiciulis,[49] S. Vallecorsa,[19] A. Varganov,[34] E. Vataga,[37] G. Velev,[16] G. Veramendi,[23] V. Veszpremi,[48] R. Vidal,[16] I. Vila,[11] R. Vilar,[11] T. Vine,[30] I. Vollrath,[33] I. Volobouev,[28] G. Volpi,[46] F. Würthwein,[9] P. Wagner,[53] R. G. Wagner,[2] R.L. Wagner,[16] W. Wagner,[25] R. Wallny,[8] T. Walter,[25] Z. Wan,[52] S.M. Wang,[1] A. Warburton,[33] S. Waschke,[20] D. Waters,[30] W.C. Wester III,[16] B. Whitehouse,[56] D. Whiteson,[45] A.B. Wicklund,[2] E. Wicklund,[16] G. Williams,[33] H.H. Williams,[45] P. Wilson,[16] B.L. Winer,[39] P. Wittich,[16] S. Wolbers,[16] C. Wolfe,[13] T. Wright,[34] X. Wu,[19] S.M. Wynne,[29] A. Yagil,[16] K. Yamamoto,[41] J. Yamaoka,[52] T. Yamashita,[40] C. Yang,[60] U.K. Yang,[13] Y.C. Yang,[27] W.M. Yao,[28] G.P. Yeh,[16] J. Yoh,[16] K. Yorita,[13] T. Yoshida,[41] G.B. Yu,[49] I. Yu,[27] S.S. Yu,[16] J.C. Yun,[16] L. Zanello,[51] A. Zanetti,[54] I. Zaw,[21] F. Zetti,[46] X. Zhang,[23] J. Zhou,[52] and S. Zucchelli[5]

(CDF Collaboration)

[1]*Institute of Physics, Academia Sinica, Taipei, Taiwan 11529, Republic of China*

[2]*Argonne National Laboratory, Argonne, Illinois 60439*

[3]*Institut de Fisica d'Altes Energies, Universitat Autonoma de Barcelona, E-08193, Bellaterra (Barcelona), Spain*

[4]*Baylor University, Waco, Texas 76798*

[5]*Istituto Nazionale di Fisica Nucleare, University of Bologna, I-40127 Bologna, Italy*

[6]*Brandeis University, Waltham, Massachusetts 02254*

[7]*University of California, Davis, Davis, California 95616*

[8]*University of California, Los Angeles, Los Angeles, California 90024*

[9]*University of California, San Diego, La Jolla, California 92093*

[10]*University of California, Santa Barbara, Santa Barbara, California 93106*

[11] Instituto de Fisica de Cantabria, CSIC-University of Cantabria, 39005 Santander, Spain
[12] Carnegie Mellon University, Pittsburgh, PA 15213
[13] Enrico Fermi Institute, University of Chicago, Chicago, Illinois 60637
[14] Joint Institute for Nuclear Research, RU-141980 Dubna, Russia
[15] Duke University, Durham, North Carolina 27708
[16] Fermi National Accelerator Laboratory, Batavia, Illinois 60510
[17] University of Florida, Gainesville, Florida 32611
[18] Laboratori Nazionali di Frascati, Istituto Nazionale
di Fisica Nucleare, I-00044 Frascati, Italy
[19] University of Geneva, CH-1211 Geneva 4, Switzerland
[20] Glasgow University, Glasgow G12 8QQ, United Kingdom
[21] Harvard University, Cambridge, Massachusetts 02138
[22] Division of High Energy Physics, Department of Physics,
University of Helsinki and Helsinki Institute of Physics, FIN-00014, Helsinki, Finland
[23] University of Illinois, Urbana, Illinois 61801
[24] The Johns Hopkins University, Baltimore, Maryland 21218
[25] Institut für Experimentelle Kernphysik,
Universität Karlsruhe, 76128 Karlsruhe, Germany
[26] High Energy Accelerator Research Organization (KEK), Tsukuba, Ibaraki 305, Japan
[27] Center for High Energy Physics: Kyungpook National University,
Taegu 702-701, Korea; Seoul National University, Seoul 151-742,
Korea; and SungKyunKwan University, Suwon 440-746, Korea
[28] Ernest Orlando Lawrence Berkeley National Laboratory, Berkeley, California 94720
[29] University of Liverpool, Liverpool L69 7ZE, United Kingdom
[30] University College London, London WC1E 6BT, United Kingdom
[31] Centro de Investigaciones Energeticas
Medioambientales y Tecnologicas, E-28040 Madrid, Spain
[32] Massachusetts Institute of Technology, Cambridge, Massachusetts 02139
[33] Institute of Particle Physics: McGill University, Montréal,
Canada H3A 2T8; and University of Toronto, Toronto, Canada M5S 1A7
[34] University of Michigan, Ann Arbor, Michigan 48109
[35] Michigan State University, East Lansing, Michigan 48824

[36] *Institution for Theoretical and Experimental Physics, ITEP, Moscow 117259, Russia*

[37] *University of New Mexico, Albuquerque, New Mexico 87131*

[38] *Northwestern University, Evanston, Illinois 60208*

[39] *The Ohio State University, Columbus, Ohio 43210*

[40] *Okayama University, Okayama 700-8530, Japan*

[41] *Osaka City University, Osaka 588, Japan*

[42] *University of Oxford, Oxford OX1 3RH, United Kingdom*

[43] *University of Padova, Istituto Nazionale di Fisica Nucleare, Sezione di Padova-Trento, I-35131 Padova, Italy*

[44] *LPNHE, Universite Pierre et Marie Curie/IN2P3-CNRS, UMR7585, Paris, F-75252 France*

[45] *University of Pennsylvania, Philadelphia, Pennsylvania 19104*

[46] *Istituto Nazionale di Fisica Nucleare Pisa, Universities of Pisa, Siena and Scuola Normale Superiore, I-56127 Pisa, Italy*

[47] *University of Pittsburgh, Pittsburgh, Pennsylvania 15260*

[48] *Purdue University, West Lafayette, Indiana 47907*

[49] *University of Rochester, Rochester, New York 14627*

[50] *The Rockefeller University, New York, New York 10021*

[51] *Istituto Nazionale di Fisica Nucleare, Sezione di Roma 1, University of Rome "La Sapienza," I-00185 Roma, Italy*

[52] *Rutgers University, Piscataway, New Jersey 08855*

[53] *Texas A&M University, College Station, Texas 77843*

[54] *Istituto Nazionale di Fisica Nucleare, University of Trieste/ Udine, Italy*

[55] *University of Tsukuba, Tsukuba, Ibaraki 305, Japan*

[56] *Tufts University, Medford, Massachusetts 02155*

[57] *Waseda University, Tokyo 169, Japan*

[58] *Wayne State University, Detroit, Michigan 48201*

[59] *University of Wisconsin, Madison, Wisconsin 53706*

[60] *Yale University, New Haven, Connecticut 06520*

Abstract

A measurement of the inclusive bottom jet cross section is presented for events containing a Z boson in $p\bar{p}$ collisions at $\sqrt{s} = 1.96$ TeV using the Collider Detector at Fermilab. Z bosons are identified in their electron and muon decay modes, and b jets with $E_T > 20$ GeV and $|\eta| < 1.5$ are identified by reconstructing a secondary decay vertex. The measurement is based on an integrated luminosity of about 330 pb^{-1}. A cross section times branching ratio of $\sigma(Z + b\,\text{jets}) \times \mathcal{B}(Z \to \ell^+\ell^-) = 0.93 \pm 0.36$ pb is found, where $\mathcal{B}(Z \to \ell^+\ell^-)$ is the branching ratio of the Z boson or γ^* into a single flavor dilepton pair (e or μ) in the mass range between 66 and 116 GeV/c^2. The ratio of b jets to the total number of jets of any flavor in the Z sample, within the same kinematic range as the b jets, is $2.36 \pm 0.92\%$. Here, the uncertainties are the quadratic sum of statistical and systematic uncertainties. Predictions made with NLO QCD agree, within experimental and theoretical uncertainties, with these measurements.

I. INTRODUCTION

The measurement of the $Z + b$ jet production cross section provides an important test of quantum-chromodynamics (QCD) calculations [1]. The cross section is sensitive to the b quark density in the proton and thus tests the perturbative calculations of this quantity. A precise knowledge of the b quark density is essential to accurately predict the production of particles that couple strongly to b quarks including Higgs bosons (h) within supersymmetry models ($gb \to hb$, $bb \to h$) [2, 3] or single top production [4] within the standard model ($qb \to q't$ and $gb \to Wt$). The $Z + b$ jet cross section is also an important test of the background predictions to standard model Higgs boson production in association with a Z boson, $ZH \to Zb\bar{b}$ [5].

The Z cross section [6–8] and Z+jets cross section [9] have been measured at the Tevatron. Next to leading order (NLO) QCD calculations are found to describe the data. In this paper, the first measurement of the b jet cross section for events with a Z boson using the Collider Detector at Fermilab (CDF) [10] is reported. A similar measurement has been made recently by the DØ collaboration [11].

The dominant production diagrams are $gb \to Zb$ and $q\bar{q} \to Zb\bar{b}$: in NLO calculations they contribute about 65% and 35%, respectively. At present the b quark density is derived from the gluon distribution [12] and agrees well with the available measurements of the contribution to the proton structure function F_2 for $Q^2 < 1,000$ GeV^2 [13], where Q^2 is the momentum transfer squared. The measurement reported in this paper is sensitive to parton densities at higher values with Q^2 approximately equal to the square of the Z mass (M_Z).

The analysis uses Run II $p\bar{p}$ collision data from CDF taken up to September 2004 at a center of mass energy of $\sqrt{s} = 1.96$ TeV. The measurement is made by searching for pairs of electrons or muons with an invariant mass consistent with M_Z and jets which contain a displaced secondary vertex consistent with the decay of a long-lived bottom hadron. The light (u, d, s, and gluon) and charm (c) jets remaining after this vertex requirement are distinguished from the b jets using the mass distribution of the charged particles forming the secondary vertex. This technique exploits the larger mass of the b quark compared with light and c quarks. The Z cross section is defined to include the irreducible Drell-Yan contribution $\gamma^* \to \ell^+\ell^-$ within the dilepton invariant mass range $66 < M_{\ell\ell} < 116$ GeV/c^2. Note that this cross section is numerically only 0.4% higher than the inclusive Z cross

section independent of the mass range [6]. The $Z + b$ jet production cross section is defined to be proportional to the number of b jets with jet tranverse energy $E_T^{\rm jet} > 20$ GeV and pseudorapidity $|\eta^{\rm jet}| < 1.5$ contained in events with a Z boson.

In Section II a brief description of the CDF detector is given, and in Section III the Monte Carlo simulation is described. Section IV summarizes the event selection and the background sources. In Section V the fraction of b jets within the data sample is determined. In Section VI the method to measure the cross section is described, and in Section VII the sources of systematic uncertainties are discussed. The results of the measurement are given in Section VIII, and a conclusion is presented in Section IX.

II. THE CDF II DETECTOR

The CDF II detector is described in detail elsewhere [10]. It is a general purpose, nearly hermetic detector situated around the $p\bar{p}$ collision point. A coordinate system is used, in which θ is the polar angle with respect to the proton beam direction, ϕ is the azimuthal angle and $\eta = -\ln\tan(\theta/2)$ is the pseudorapidity. The transverse energy and transverse momentum of a particle is defined as $E_T = E\sin\theta$ and $p_T = p\sin\theta$, respectively, where E is the energy measured by the calorimeter and p is the momentum measured in the tracking system. The missing transverse energy vector is defined as $\vec{\not\!\!E}_T = -\sum_i E_T^i \vec{n}_i$, where $\vec{n}_i$ is a unit vector that points from the interaction vertex to the center of the ith calorimeter tower in the transverse plane and E_T^i is the transverse energy of the ith tower. The quantity $\not\!\!E_T$ is the magnitude of $\vec{\not\!\!E}_T$, which is corrected for all identified muons in an event [7].

The transverse momenta of charged particles are measured by an eight-layer silicon strip detector [14–16] and the central outer tracker (COT), a 96-layer drift chamber [17] located inside a solenoid that provides a 1.4 T magnetic field. The innermost layer of the silicon detector is located on the beryllium beampipe at a radius of 1.5 cm, and the outermost layer is located at 28 cm. The silicon detector provides tracking in the pseudorapidity region $|\eta| < 2$, with partial coverage up to $|\eta| < 2.8$. The single hit resolution is about 11 μm. Located outside of the silicon detector, the COT is a 3.1 m long, open-cell drift chamber with an active tracking region extending radially from 41 cm to 137 cm. The COT provides coverage for $|\eta| < 1$. For tracks with $p_T > 1.5$ GeV/c and silicon hits the resolution on the impact parameter is about 34 μm [18], including the transverse size of the beam of

about 25 μm.

Located outside the solenoid, a segmented sampling calorimeter is used for the measurement of particle energies. The central part of the calorimeter covers the region $|\eta| < 1.1$ [19, 20], and the forward part of the calorimeter consists of two identical detectors covering $1.1 < |\eta| < 3.6$ [21]. The central calorimeter uses lead-scintillator sampling in the electromagnetic compartment and steel-scintillator sampling in the hadronic compartment. It is instrumented with proportional strip and wire chambers (central electromagnetic shower maximum detector, CES). They are located at a depth of about six radiation lengths where the lateral profile of electromagnetic showers is expected to be maximal and have a segmentation of 1.5 cm. The forward calorimeter uses lead-scintillator sampling for the electromagnetic compartment and iron-scintillator for the hadronic compartment. Further details about the calorimeters can be found in Ref. [22].

Drift chambers, located outside the central hadron calorimeters and behind 60 cm of iron shielding, detect muons with $|\eta| < 0.6$ [23]. Additional drift chambers and scintillation counters detect muons in the regions $0.6 < |\eta| < 1.0$ and $1.0 < |\eta| < 1.5$. Gas Cherenkov counters [24] measure the average number of $p\bar{p}$ inelastic collisions per bunch crossing to determine the luminosity.

III. MONTE CARLO SIMULATION

A Monte Carlo simulation is used to correct for inefficiencies due to the selection requirements and detector effects. The Monte Carlo generator PYTHIA v6.2 [25] is used to generate the Drell-Yan signal and the background processes, using CTEQ5L parton density functions (PDFs) [26]. An underlying event model that describes the interactions of the spectator partons and initial state QCD radiation has been included in the generation. This model has been tuned to describe the Tevatron data [22, 27]. The decays of the b hadrons are generated by the Monte Carlo generator QQ v9.1 [28]. The CDF detector response is simulated using a GEANT based detailed detector simulation [29, 30].

The Drell-Yan Monte Carlo samples are normalized to the next to next to leading order (NNLO) QCD cross section of 251.3 pb [31] for $66 < M_{\ell\ell} < 116$ GeV/c^2, so that comparisons with the data can be made. For $t\bar{t}$ and ZZ processes, which contribute to the background, the NLO QCD cross sections are used for the normalization: $\sigma_{t\bar{t}} = 6.77$ pb [32] and $\sigma_{ZZ} =$

1.4 pb [33].

Simulated events are reconstructed in the same manner as the data events, and the same event selection criteria are applied.

IV. EVENT SELECTION AND BACKGROUND

A. Event Selection

Z bosons are detected in their decays into two electrons or two muons with an invariant mass of the two leptons $M_{\ell\ell}$ ($\ell = e$ or μ) between 66 and 116 GeV/c^2. The trigger requirements and the lepton selection follow closely those described in detail in Ref. [7].

Electrons are triggered by requiring a cluster of electromagnetic energy with $E_T > 18$ GeV and $|\eta| < 1.1$ matched to a track with $p_T > 10$ GeV/c. Further requirements are made on position matching and the shower shape in the CES. At least one trigger electron candidate is required. The second electron candidate can either be in the central or forward calorimeter, and looser identification criteria are imposed. For forward electron candidates no matching track is required. All electron candidates are required to be isolated from other calorimeter energy deposits [7].

Muons are triggered by requiring a track with $p_T > 18$ GeV/c and $|\eta| < 1.0$ and a track segment in the muon chambers that matches the extrapolated position of the track. At least one muon candidate that satisfies the trigger requirements is required. The other muon candidate is not required to have signals in the muon chambers. All muon candidates are required to have a calorimeter energy deposit consistent with that of a muon and to be isolated from other energy depositions [6, 7]. The two highest p_T muon candidates are required to have opposite electric charges.

Candidate Z boson events are selected if $66 < M_{\ell\ell} < 116$ GeV/c^2. A total of 27,659 candidate events are observed in the electron channel and 15,698 events in the muon channel.

Having selected an event with a Z boson candidate, jets with $E_T^{\rm jet} > 20$ GeV and $|\eta^{\rm jet}| < 1.5$ are searched for. Jets are defined by a cone jet algorithm with a cone size $R = \sqrt{(\Delta\eta)^2 + (\Delta\phi)^2} = 0.7$ [22]. The jet energy is corrected to the hadron level energy. The hadron level energy is defined to include all particles from the $p\bar{p}$ collision within the jet cone, including particles from the hard scatter, multiple parton-parton interactions, and

beam remnants. The jet energy is also corrected for particles produced in additional $p\bar{p}$ interactions, reconstructed in the same bunch crossing. The jets are not corrected to the parton level to be independent of the Monte Carlo modeling of this correction.

Events must satisfy either $\not\!\!E_T < 25$ GeV or $H_T < 150$ GeV, where H_T is the scalar sum of $\not\!\!E_T$ and the transverse energies of all leptons and jets in the event [34]. This requirement reduces background from $t\bar{t}$ events in which the t decays to Wb and both the W bosons decay leptonically ($W \to l\nu$) by about 80%, while reducing the signal by only 4%, as determined from Monte Carlo simulation.

A b jet is defined as any jet that has at least one b hadron within a cone of 0.7 around the jet axis. In this analysis a b jet is identified through the presence of a displaced vertex within the jet arising from the decay of the long-lived bottom hadron. The algorithm used was optimized for the measurement of the top quark production cross section [35] but found to give adequate efficiency and purity for the present analysis. A jet that has a reconstructed displaced vertex is called a "b tagged" jet. The displaced vertex algorithm uses a two-pass approach to find a secondary vertex. In the first pass an attempt is made to reconstruct a secondary vertex using one track with $p_T > 1.0$ GeV/c and two or more additional tracks with $p_T > 0.5$ GeV/c, and all tracks are required to have an impact parameter significance $d_0/\sigma_{d_0} > 2.5$. Here, d_0 is the minimum distance between the track and the primary vertex in the plane transverse to the beam direction and has uncertainty σ_{d_0}. If the first pass is unsuccessful, a second pass is made using two tracks with $p_T > 1.5$ GeV/c for one track, $p_T > 1.0$ GeV/c for the other and $d_0/\sigma_{d_0} > 3$ for both. The jet is labeled as a tag if the transverse displacement significance $|L_{2D}|/\sigma_{L_{2D}} > 7.5$. Here, L_{2D} is the distance from the primary vertex to the secondary vertex in the plane transverse to the beam direction projected onto the jet axis, and $\sigma_{L_{2D}}$ is the estimated uncertainty. The distance L_{2D} is defined as positive if the angle between the transverse displacement and the jet direction is less than 90°, and as negative otherwise. A *positive tag* has positive L_{2D}, and a *negative tag* has negative L_{2D}.

The b tagging efficiency is determined as a function of $E_T^{\rm jet}$ and $\eta^{\rm jet}$ from a separate data sample of about 28,000 dijet events, where one of the jets has a reconstructed semileptonic b or c decay [35]. The ratio of the efficiency in data to that in Monte Carlo simulation is found to be 0.91 ± 0.06. The average data b tagging efficiency for jets in this analysis is $33 \pm 2\%$.

In total, 115 tagged jets are selected, 60 in the electron channel and 55 in the muon channel. This compares with a Monte Carlo estimate of 69 in the electron and 45 in the muon channel. The Monte Carlo estimate includes the Drell-Yan contribution, which has been scaled by the factors obtained in the fit to the secondary vertex mass (see Section V), and the backgrounds listed in Section IV B. Out of the 115 tagged jets 16 are negatively tagged compared with a Monte Carlo estimate of 16.7. One event contains two positively tagged b jets compared with a Monte Carlo expectation of 1.46.

B. Backgrounds

Backgrounds to $Z + b$ production can arise from misidentified leptons, from genuine leptons and b jets coming from other processes, or from light jets or c jets that are misidentified as b jets. The first two background sources are discussed in this section, and the latter is discussed in section V.

The background in which one or both reconstructed electrons in the $Z \rightarrow e^+e^-$ channel are misidentified from other particles in the final state is estimated from the data. The probability that a jet will pass all electron identification criteria is determined from several inclusive jet samples. These samples have negligible prompt electron content. The probabilities are parameterized as a function of $E_T^{\rm jet}$ and are on average 0.1% for central jets and 1.5% for forward jets. Because an associated track is not required for a forward electron, the misidentification probability is much higher than for central electrons.

A sample of events in which exactly one trigger electron is reconstructed is now taken. The trigger electron is paired with any other jet in the event such that the invariant mass of the electron and the jet, with the jet energy corrected as if it were an electron, lies within the Z mass window. A weight, which equals the jet misidentification probability, is assigned to the jet. The total background to inclusive Z production is then the sum of all weights. If there is more than one jet in the event that forms an invariant mass within the mass window of the Z, each combination is used. Background distributions are derived by weighting the electron + jets distributions with the weights. The background for Z+jets ($Z + b$ jets) is the sum of those weights for events which contain at least one jet (b jet) in addition to the one paired with the electron.

Using this method, a background contribution of 3.1 ± 1.5 b tagged jets is estimated

within the Z mass window.

Background in the $Z \to \mu^+\mu^-$ channel in which the electric charges of the two muon candidates are uncorrelated is estimated from events with two reconstructed muon candidates that have the same electric charge [7]. This background comes from events in which one or both muon candidates arise from hadron decays or events in which hadrons in the final state are misidentified as muons. Due to the low statistics of the events with a b tagged jet, the fractional contribution of this background is estimated as the observed ratio of generic jets (i.e., any jet regardless of which quark flavor or gluon it originated from) with a like-sign Z candidate to those with an unlike-sign Z candidate. The number of b tagged jets from this background source is estimated to be 0.24 ± 0.12. This number is in agreement with the zero tagged jets with a like sign Z candidate observed in the data.

The background from other processes is estimated from Monte Carlo simulations. The production of $t\bar{t}$ pairs is found to contribute 0.25 ± 0.05 (0.24 ± 0.05) tagged jets to the electron (muon) channel. The production of ZZ is found to contribute 0.36 ± 0.07 (0.28 ± 0.06) tagged jets to the electron (muon) channel. Backgrounds from other processes such as WW, WZ, $b\bar{b}$ production or $Z \to \tau^+\tau^-$ are estimated to be negligible.

The invariant mass of the dilepton pair is shown in Figure 1 for events with at least one generic jet with $E_T^{\rm jet} > 20$ GeV and $|\eta^{\rm jet}| < 1.5$. The data are compared with the expected Drell-Yan and estimated background contributions. Good agreement is observed near M_Z and in the tails. Figure 2 shows the dilepton invariant mass for events with at least one positively tagged jet in the same kinematic range. The data are well modeled by the simulation, and a clear Z signal is also observed in this sample.

V. FRACTION OF b JETS

The fraction of b jets in the tagged jet sample is estimated by performing a fit to the invariant mass of all charged tracks attached to the secondary vertex M_S [36]. On average b jets have a larger M_S than c jets or light jets due to the larger mass of b hadrons. The M_S distribution for both positively and negatively tagged jets is used, in order to better discriminate between heavy and light jets, since jets with a genuine secondary vertex overwhelmingly have positive tags, whereas jets with a false secondary vertex may have positive or negative tags. In addition using the negative tags in the fit allows a better separation

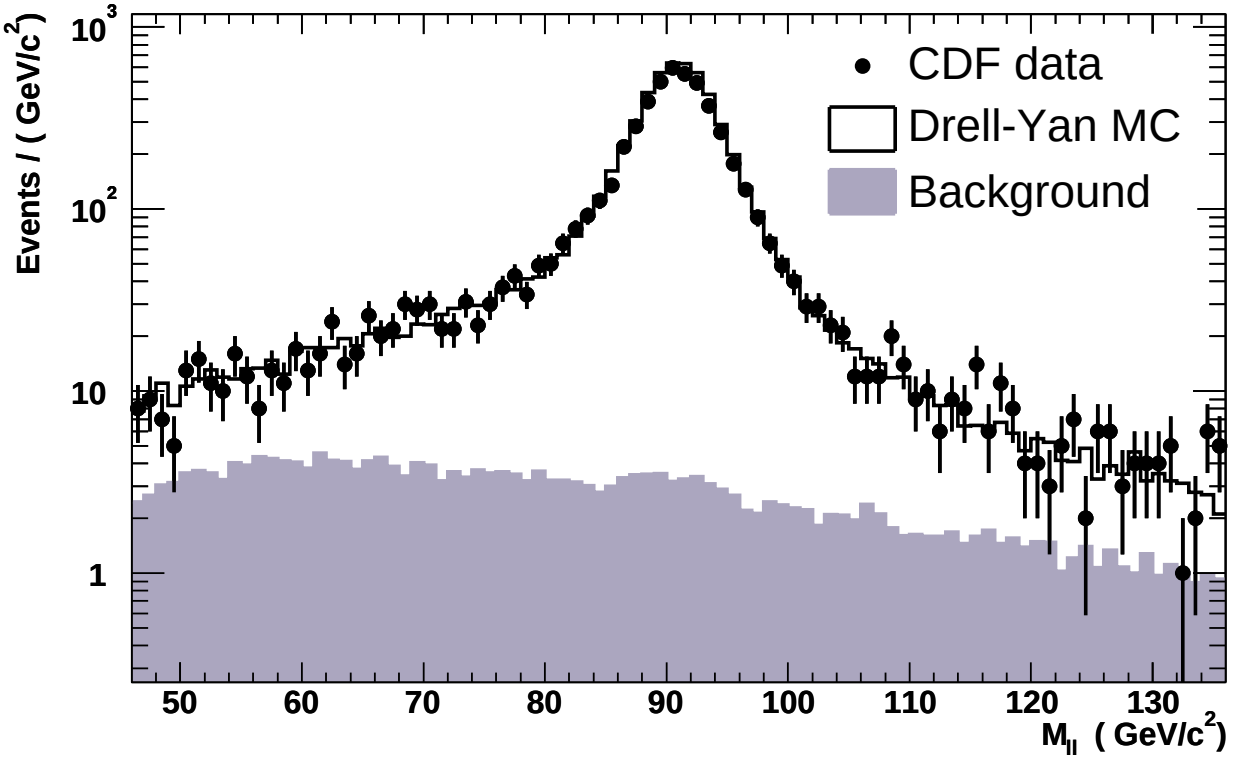

Figure 1: The invariant mass of the dilepton pair for the sample with jets with $E_T^{\rm jet} > 20$ GeV and $|\eta^{\rm jet}| < 1.5$ compared with the expectation from signal and background sources. The Drell-Yan Monte Carlo has been normalized to the luminosity of the data sample assuming the NNLO Drell-Yan cross section.

of the charm and light quark contributions that have similar M_S distribution for positively tagged jets.

The M_S distributions for positively and negatively tagged data jets is shown in Figure 3. The distributions of M_S for b, c, and light jet events are taken from the Monte Carlo simulation. The Monte Carlo light jet distribution has been corrected using data as described below.

It is important to ensure that the simulation models the M_S distributions well. The M_S distributions are affected by the tracking efficiency, the charged particle multiplicity of the b hadron decay, and the fraction of jets with two b or c hadrons. Systematic uncertainties have been assigned to each of these contributions (see Section VII), and the M_S distribution

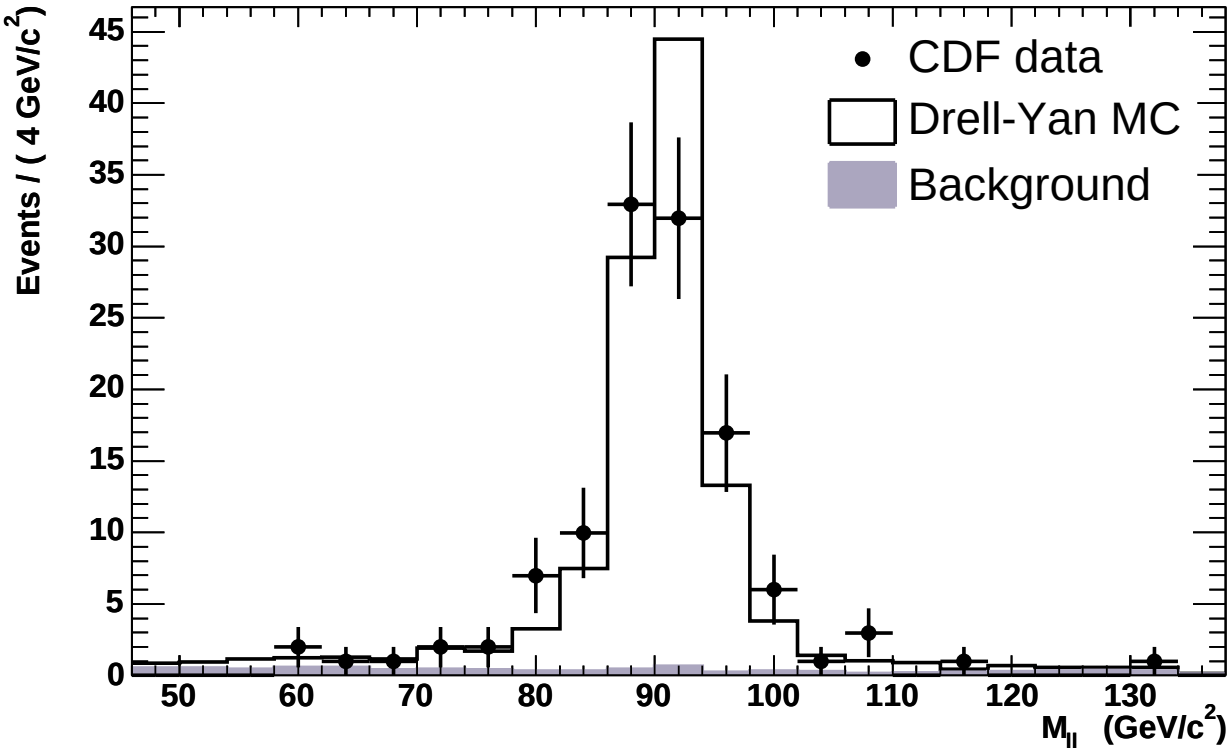

Figure 2: The invariant mass of the dilepton pair for the sample with positively tagged jets with $E_T^{\rm jet} > 20$ GeV and $|\eta^{\rm jet}| < 1.5$ compared with the expectation from signal and background sources. The Drell-Yan Monte Carlo has been scaled by the factors determined in Section V.

in a Monte Carlo simulation of b jets has been compared with the dijet sample used to determined the b efficiency (see Section IV). The simulation is found to describe the data within the uncertainties quoted [37].

The number of positive tags in light quark jets is larger than the number of negative tags due to long lived particles, such as K_S^0 and Λ, and due to vertices produced by nuclear interactions of particles with material in their path [35]. The current simulation may not describe these effects accurately. In order to investigate these effects, a sample of approximately 13,000 $\gamma +$ jet data events is taken, with jets in the same kinematic range as for the $Z + b$ jets selection. This sample was chosen since it has higher statistics than and a similar event topology as the $Z + b$ jets sample. The M_S distribution of the $\gamma +$ jet data is obtained separately for positive and negative tags. The fraction of light, c, and b jets in

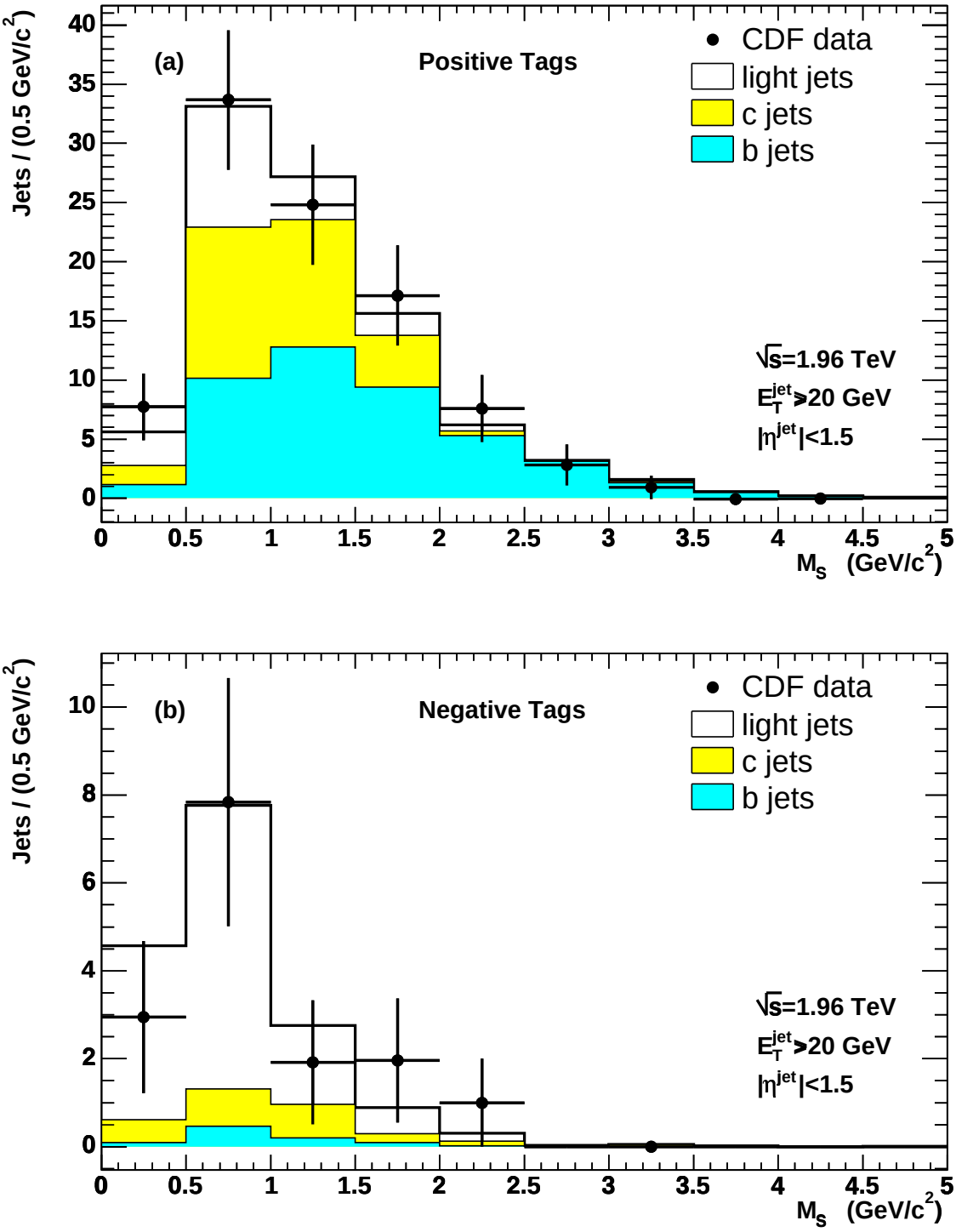

Figure 3: The mass at the secondary vertex, M_S, for (a) positively and (b) negatively tagged jets with $E_T^{\rm jet} > 20$ GeV and $|\eta^{\rm jet}| < 1.5$. The non-Drell-Yan background has been subtracted from the data. The data are compared with the sum of the light, c and b Monte Carlo templates after being scaled by the factors ρ_l, ρ_c, and ρ_b, respectively. The open white area represents the light quark template, the lightly shaded are the c quark template and the dark shaded are the b quark template.

each sample is determined using Monte Carlo distributions as templates and performing a likelihood fit, similar to the one described below, in which the normalization of each Monte Carlo template is allowed to vary. It is found that the ratio of positive to negative tags for light jets in the data is 1.49, compared with the expectation from the Monte Carlo of 1.93. To correct for the difference between the data and the Monte Carlo simulation, the Monte Carlo light negative tagged jets are increased by a factor of $1.93/1.49 = 1.30$. This reweighted template shape is taken for the central value, and the full difference from unity, $\pm 30\%$, is taken as the systematic uncertainty.

A binned maximum likelihood fit using Poisson statistics is performed to the M_S distributions of the positively and negatively tagged jets in the Z sample for range $M_S < 3.5(1)$ GeV/c^2 for positively (negatively) tagged jets. The range is chosen in order to have enough statistics for the fit. The Monte Carlo distributions are taken as templates and scaled by factors ρ_b, ρ_c, and ρ_l for b, c, and light jets, respectively. The data distribution is used after subtraction of the non-Drell-Yan background as estimated in Section IV B. The quantity ρ_b is thus the number of fitted reconstructed signal b jets in data divided by the number in the simulation. Only statistical errors from the data and Monte Carlo are used in the fit. The fit takes into account the Monte Carlo statistical errors using the method described in Ref. [38]. The fit gives values of $\rho_b = 0.93 \pm 0.29$, $\rho_c = 1.69 \pm 0.94$ and $\rho_l = 1.36 \pm 0.53$. The correlation coefficient between ρ_b and ρ_c is -0.68 and between ρ_b and ρ_l is 0.10.

The number of b jets in the Z sample after subtracting the background contributions is estimated to be $N_{\rm Data}(Z + b\,\text{jets}) = 45 \pm 14$. A check is performed by fitting only positively tagged jets, and good agreement is obtained with a value of $\rho_b = 0.95 \pm 0.31$.

VI. CROSS SECTION

The inclusive b jet cross section $\sigma(Z + b\,\text{jets})$ is proportional to the number of b jets with $E_T^{\rm jet} > 20$ GeV and $|\eta^{\rm jet}| < 1.5$ and is defined for dilepton masses $66 < M_{\ell\ell} < 116$ GeV/c^2. The branching fraction $\mathcal{B}(Z \to \ell^+\ell^-)$ is defined for a single lepton flavor.

A ratio method is used to extract the cross section. In doing so use can be made of the uncertainties estimated for the inclusive Z cross section measurement [7] for the lepton and trigger selection. First a measurement is made of the ratio of the $Z + b$ jet cross section to the total Z cross section:

$$\frac{\sigma(Z+b\,\text{jets})}{\sigma(Z)} = \frac{N_{\text{Data}}(Z+b\,\text{jets})/\epsilon(Z+b\,\text{jets})}{N_{\text{Data}}(Z)/\epsilon(Z)}, \tag{1}$$

where $N_{\text{Data}}(Z+b\,\text{jets})$ is the fitted number of b jets (see Section V) and $N_{\text{Data}}(Z)$ is the total number of events with a lepton pair in the mass range $66 < M_{\ell\ell} < 116$ GeV/c^2 in the data. In both cases the number of data events is taken after subtraction of the background contributions (see Section IV B). The efficiencies of the $Z+b\,$jet and the Z boson selections are $\epsilon(Z+b\,\text{jet}) = 7.7\%$ and $\epsilon(Z) = 27\%$, respectively. They are determined from PYTHIA Monte Carlo simulation and are corrected for any differences from the data. The ratio $\epsilon(Z+b\,\text{jets})/\epsilon(Z)$ is also determined using HERWIG v6.5 [39] and a similar result is obtained (0.286 for HERWIG compared with 0.285 for PYTHIA).

The cross section is then calculated as:

$$\sigma(Z+b\,\text{jets}) \times \mathcal{B}(Z\to\ell^+\ell^-) = \frac{\sigma(Z+b\,\text{jets})}{\sigma(Z)} \cdot \sigma_{\text{CDF}}(Z) \times \mathcal{B}(Z\to\ell^+\ell^-), \tag{2}$$

where $\sigma_{\text{CDF}}(Z) \times \mathcal{B}(Z\to\ell^+\ell^-) = 254.9 \pm 3.3(\text{stat.}) \pm 4.6(\text{syst.}) \pm 15.2(\text{lum.})$ pb is the CDF measurement of the Z production cross section times branching fraction for a single lepton flavor [6].

A measurement is also made of the ratio of the $Z+b$ jets cross section to the $Z+$ generic jets cross section to measure the fraction of jets that contain at least one b hadron. The $Z+$ generic jets cross section is proportional to the number of generic jets with $E_T^{\text{jet}} > 20$ GeV and $|\eta^{\text{jet}}| < 1.5$. The ratio of the $Z+b$ jets to $Z+$ generic jets cross section is obtained from the data as:

$$\frac{\sigma(Z+b\,\text{jets})}{\sigma(Z+\text{ jets})} = \frac{N_{\text{Data}}(Z+b\,\text{jets})/\epsilon(Z+b\,\text{jets})}{N_{\text{Data}}(Z+\text{jets})/\epsilon(Z+\text{jets})}, \tag{3}$$

where $N_{\text{Data}}(Z+\text{jets})$ is the number of generic data jets for events with a lepton pair within the Z mass window after background subtraction and $\epsilon(Z+\text{jets}) = 24\%$ is the efficiency of the $Z+$jet selection.

The validity of the kinematic distributions in the Monte Carlo simulation was checked by comparing the transverse energy and pseudorapidity distributions for generic jets and for the positively b tagged jets. These distributions, which are shown in Figure 4 for generic

jets and in Figure 5 for b jets, demonstrate that PYTHIA describes the data well and thus may be used to correct the data.

VII. SYSTEMATIC UNCERTAINTIES

The total systematic uncertainty on the measurement is estimated by adding the uncertainties described in this section in quadrature.

The uncertainty on the jet energy scale was estimated by changing the scale in the Monte Carlo simulation by the uncertainty following the procedure of Ref. [22]. An additional uncertainty of $\pm 0.6\%$ [40] is applied on the b jets to account for possible differences in the description of b jets by the Monte Carlo simulation compared with light jets.

Possible differences between the Monte Carlo simulation and data $E_T^{\rm jet}$ and $\eta^{\rm jet}$ distributions, which may arise for many reasons including uncertainties in the parton distribution functions, inadequacies in the QCD model or uncertainties in the b quark fragmentation, are accounted for in the systematic error by weighting the Monte Carlo hadron level distributions by $(E_{T\rm Had}^{\rm jet}/35)^{\pm\alpha_{E_T}}$ and $(|\eta_{\rm Had}^{\rm jet}|+0.5)^{\pm\alpha_\eta}$, respectively. Here $E_{T\rm Had}^{\rm jet}$ is the transverse energy in GeV, and $\eta_{\rm Had}^{\rm jet}$ is the pseudorapidity of the Monte Carlo hadronic jet. The values of 35 GeV and 0.5 units of pseudorapidity are arbitrary and chosen to be close to the center of the distributions. The parameter α_{E_T} is set to 0.2 (1.0) for untagged (tagged) jets. The parameter α_η is set to 0.2 (1.0) for untagged (tagged) jets. These parameters are chosen by comparing the weighted and unweighted Monte Carlo reconstructed distributions with those of the data and choosing the weight such that it is still statistically compatible with the data.

The b jet tagging efficiency has a 6.6% uncertainty [35].

Since any changes in the shapes of the light, c and b jet templates can change the value of ρ_b obtained, various possible variations of the template shapes are included in the systematic uncertainty. An uncertainty in the negative to positive light jet tag rate is estimated by weighting the negative tags of the light template by $\pm 30\%$. This is the observed difference between data and Monte Carlo simulation for the negative to positive light jet tag ratio (see section V). Since it is not *a priori* known whether the jets contain one or two heavy quarks, an uncertainty in the shape of the c (b) quark template is estimated by taking half the difference between results obtained using the templates when there is one or two c (b) hadrons

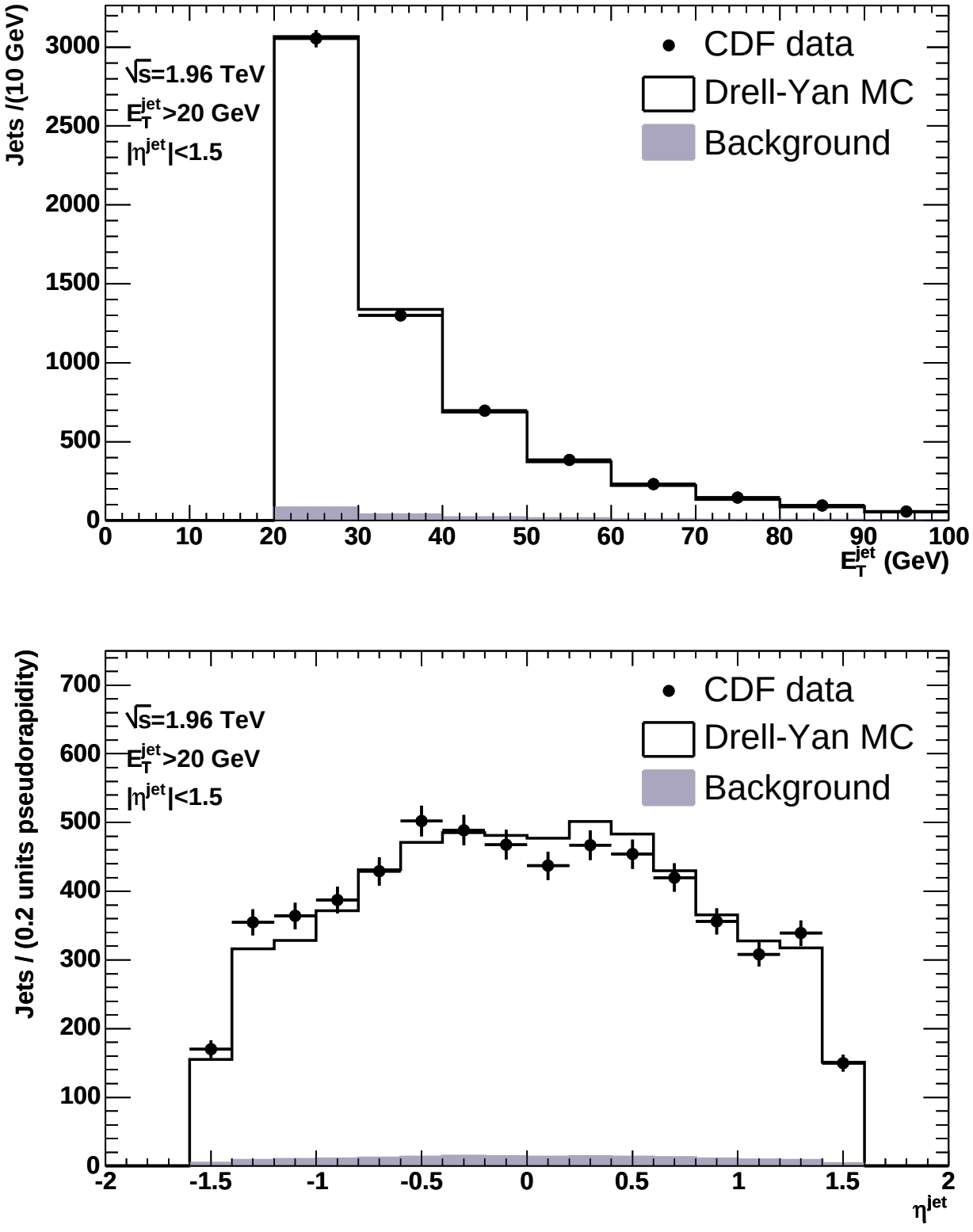

Figure 4: The $E_T^{\rm jet}$ and $\eta^{\rm jet}$ distributions for generic jets with $E_T^{\rm jet} > 20$ GeV and $|\eta^{\rm jet}| < 1.5$. The Drell-Yan Monte Carlo has been scaled such that the total number of jets in the simulation is the same as in the data.

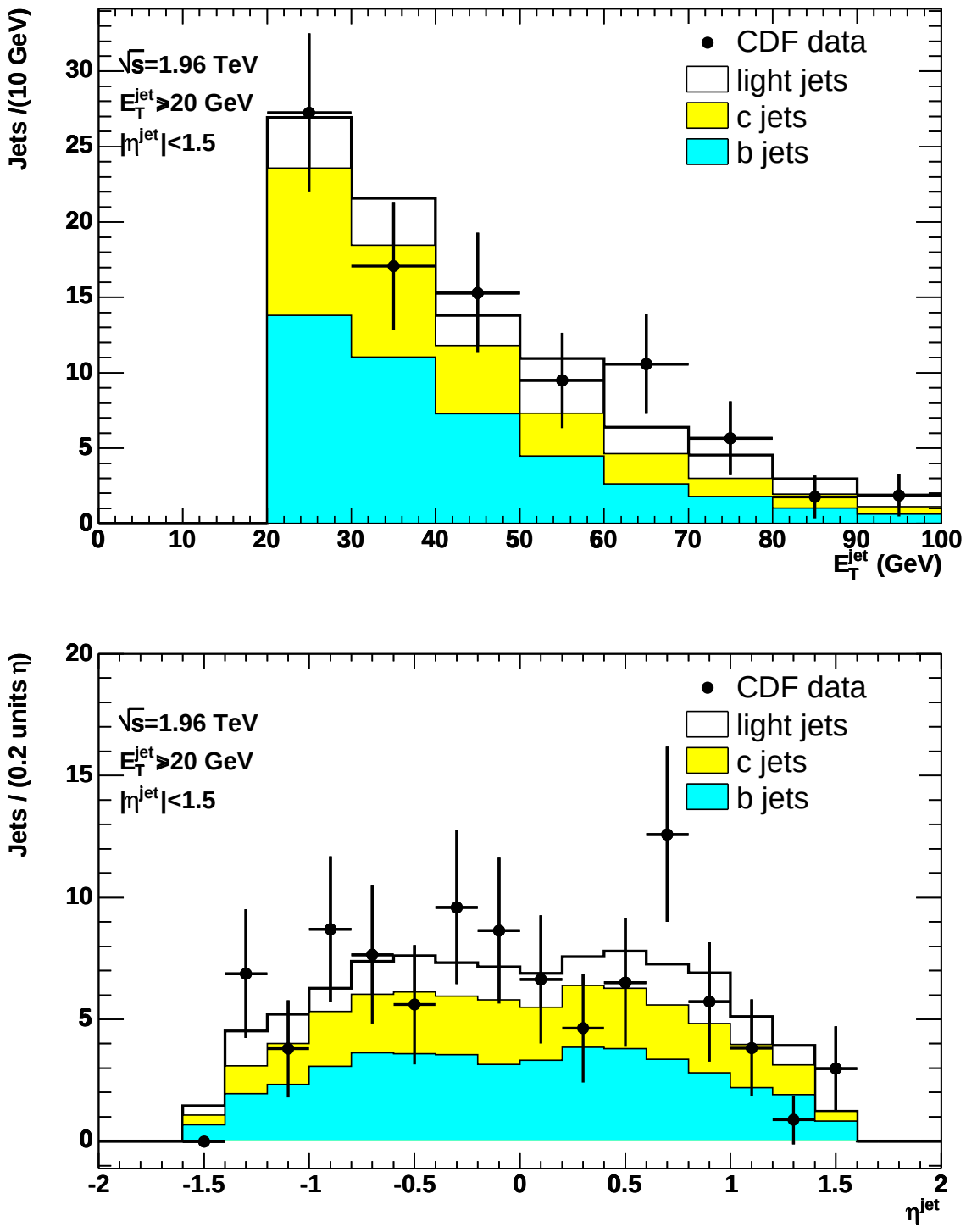

Figure 5: The $E_T^{\rm jet}$ and $\eta^{\rm jet}$ distributions for positively tagged jets with $E_T^{\rm jet} > 20$ GeV and $|\eta^{\rm jet}| < 1.5$. The non-Drell-Yan background has been subtracted from the data. The data are compared with the sum of the light, c and b contributions after being scaled by the factors ρ_l, ρ_c, and ρ_b, respectively (see Section V). The open white area represents the light quark template, the lightly shaded are the c quark template and the dark shaded are the b quark template.

within a cone of 0.7 around the jet axis. An uncertainty due to possible track reconstruction inefficiencies is estimated by recalculating templates after randomly removing 3% of the tracks in the Monte Carlo simulation. An uncertainty in the shape of the b quark template due to the uncertainty in the mean b hadron charged particle multiplicity is estimated by weighting the Monte Carlo multiplicity such that the mean changes by ± 0.15, which is the difference between Monte Carlo simulation and data measurements [41].

An uncertainty on the misidentified electron and muon backgrounds is estimated to be $\pm 50\%$ of the estimated contribution (see Section IV B). An uncertainty in the ZZ and $t\bar{t}$ backgrounds of $\pm 20\%$ is estimated. These uncertainties include the NLO cross section uncertainty estimated by varying the factorization scale by a factor two [32, 33], the cross section uncertainty due to the uncertainty on the top quark mass, and experimental uncertainties (e.g. the lepton identification and b jet tagging efficiencies).

A 1.8% uncertainty on the selection efficiency of Z events is taken from Ref. [6]. A 5.8% uncertainty is taken for the luminosity determination [42].

The effect of these contributions on the systematic uncertainty on the cross section is listed in Table I. The systematic uncertainties are evaluated separately for the cross section ratio measurements and are also included in Table I. The total systematic uncertainty on the cross section is 22% compared with a statistical precision of 31%. The largest uncertainty arises from the assumed Monte Carlo $E_T^{\rm jet}$ distribution and will be reduced with higher data statistics to constrain this distribution.

VIII. RESULTS

The b jet cross section for events with $66 < M_{\ell\ell} < 116$ GeV/c^2 and $E_T^{\rm jet} > 20$ GeV and $|\eta^{\rm jet}| < 1.5$ is measured to be

$$\sigma(Z + b\,\text{jets}) \times \mathcal{B}(Z \to \ell^+\ell^-) = 0.93 \pm 0.29(\text{stat.}) \pm 0.21(\text{syst.})\ \text{pb}.$$

The theoretical prediction of 0.45 ± 0.07 pb is consistenet with the measurement. The theoretical cross section and the ratios listed below were evaluated at NLO using MCFM [1, 43] with the parton distribution functions from CTEQ6M [44]. The factorization and renormalization scales were set to M_Z. The uncertainty on the NLO prediction includes the uncertainty arising from the choice of these scales, which were varied from $M_Z/2$ to $2M_Z$,

Table I: The systematic uncertainties on the cross section and ratio measurements. The total systematic uncertainty on each measurement is estimated by adding the individual uncertainties in quadrature.

Source of Uncertainty	$\delta(\sigma(Z+b\,\text{jets})$ (%)	$\delta(\sigma(Z+b\,\text{jets})/\sigma(Z))$ (%)	$\delta(\sigma(Z+b\,\text{jets})/\sigma(Z+\text{jets}))$ (%)
jet energy scale	3.9	3.9	6.7
b jet energy scale	0.2	0.2	0.2
MC η^{jet} dependence	6.6	6.6	6.6
MC E_T^{jet} dependence	16.1	16.1	16.2
b tagging efficiency	6.6	6.6	6.6
light jet template	1.8	1.8	1.8
single/double c quark in jet	2.8	2.8	2.8
single/double b quark in jet	3.6	3.6	3.6
track reconstruction efficiency	9.9	9.9	9.9
b hadron multiplicity	1.0	1.0	1.0
misidentified lepton background	1.3	0.9	0.4
other backgrounds	0.3	0.3	0.3
Z selection efficiency	1.8	–	–
luminosity	5.8	–	–
total	22.9	22.1	22.8

the uncertainty on the parton distribution functions and the uncertainty on the strong coupling constant.

The ratio of $Z+b\,\text{jets}$ production to inclusive Z production is measured to be

$$\sigma(Z+b\,\text{jets})/\sigma(Z) = 0.0037 \pm 0.0011(\text{stat.}) \pm 0.0008(\text{syst.}).$$

The PYTHIA estimate of 0.0035 and the NLO QCD calculation of 0.0019 ± 0.0003 both agree with the measured value.

The NLO QCD cross section $\sigma(Z+b\,\text{jets})$ and the ratio $\sigma(Z+b\,\text{jets})/\sigma(Z)$ do not include

the effects of underlying event and hadronization. These effects are estimated from PYTHIA to change the NLO QCD cross section and the ratio to the inclusive Z cross section by $+10\%$ for the underlying event and -1% for the hadronization.

The ratio of $Z + b$ jets production compared to $Z +$ jets production is measured to be

$$\sigma(Z + b\,\text{jets})/\sigma(Z + \text{ jets}) = 0.0236 \pm 0.0074(\text{stat.}) \pm 0.0053(\text{syst.})$$

The estimate from PYTHIA of 0.0218 and the NLO QCD calculation of 0.0181 ± 0.0027 agree with this result. The NLO QCD cross section has not been corrected for underlying event and hadronization. These effects are estimated from PYTHIA and change the value by -7% and $+1\%$, respectively. The measurement is also in agreement with the analysis from the DØ collaboration [11] of $0.021 \pm 0.004(\text{stat.})^{+0.002}_{-0.003}(\text{syst.})$, which measures the fraction of events with at least one b jet, with $P_T^{\text{jet}} > 20$ GeV/c and $|\eta^{\text{jet}}| < 2.5$, to those events with at least one generic jet within the same kinematic range. Note that in the analysis by the DØ collaboration, an NLO QCD prediction for the ratio of the $Z + b$ quark to the $Z + c$ quark production rate is assumed. This assumption results in smaller uncertainties for the DØ analysis despite the present analysis having more than twice the number of tagged b jets and similar b purity. The present analysis does not take the approach followed by the DØ collaboration in order to maintain independence of the measurement from QCD calculations.

IX. CONCLUSIONS

In conclusion, the inclusive $Z + b$ jets production cross section has been measured for jets with $E_T > 20$ GeV and $|\eta^{\text{jet}}| < 1.5$ in $p\bar{p}$ collisions at $\sqrt{s} = 1.96$ TeV at the Tevatron using CDF data with an integrated luminosity of about 330 pb^{-1}.

The $Z + b$ jets cross section times branching ratio is measured as 0.93 ± 0.36 pb for the Z decaying into a single charged lepton flavor. The ratio of the $Z + b$ jets to the $Z +$ jets cross section is $2.36 \pm 0.92\%$. This is the first measurement of the $Z + b$ jets cross section without any assumptions on the $Z + c$ jets production rate. The uncertainty is dominated by the limited statistical precision, which is expected to improve significantly in the near future.

Within current uncertainties, the theoretical predictions agree with these measurements, which are sensitive to the b quark density at high momentum transfer.

Acknowledgments

We thank the Fermilab staff and the technical staffs of the participating institutions for their vital contributions. We also thank John Campbell for his help on the theoretical prediction.

This work was supported by the U.S. Department of Energy and National Science Foundation; the Italian Istituto Nazionale di Fisica Nucleare; the Ministry of Education, Culture, Sports, Science and Technology of Japan; the Natural Sciences and Engineering Research Council of Canada; the National Science Council of the Republic of China; the Swiss National Science Foundation; the A.P. Sloan Foundation; the Bundesministerium für Bildung und Forschung, Germany; the Korean Science and Engineering Foundation and the Korean Research Foundation; the Particle Physics and Astronomy Research Council and the Royal Society, UK; the Russian Foundation for Basic Research; the Comisión Interministerial de Ciencia y Tecnología, Spain; in part by the European Community's Human Potential Programme under contract HPRN-CT-2002-00292; and the Academy of Finland.

---

[1] J. Campbell, R.K. Ellis, F. Maltoni and S. Willenbrock, Phys. Rev. D **69**, 074021 (2004).

[2] D. Dicus, T. Stelzer, Z. Sullivan and S. Willenbrock, Phys. Rev. D **59**, 094016 (1999); C. Balasz, H. J. He and C. P. Yuan, Phys. Rev. D **60**, 114001 (1999); F. Maltoni, Z. Sullivan and S. Willenbrock, Phys. Rev. D **67**, 093005 (2003).

[3] D. Choudhury, A. Datta and S. Raychoudhuri, arXiv:hep-ph/9812201; C. S. Huang and S. H. Zhou, Phys. Rev. D **60**, 075012 (1999); J. Campbell, R.K. Ellis, F. Maltoni and S. Willenbrock, Phys. Rev. D **67**, 095002 (2003).

[4] T. Stelzer, Z. Sullivan and S. Willenbrock, Phys. Rev. D **56**, 5919 (1997); T. Stelzer, Z. Sullivan and S. Willenbrock, Phys. Rev. D **58**, 094021 (1998).

[5] M. Carena *et al.*, Higgs Working Group Collaboration, arXiv:hep-ph/0010338.

[6] D. Acosta *et al.* (CDF Collaboration), Phys. Rev. Lett. **94**, 091803 (2005).

[7] A. Abulencia *et al.* (CDF Collaboration), arXiv:hep-ex/0508029, submitted to Phys. Rev. D.

[8] B. Abbott *et al.* (DØ Collaboration), Phys. Rev. D **60**, 052003 (1999).

[9] F. Abe *et al.* (CDF Collaboration), Phys. Rev. Lett. **77**, 448 (1996).

[10] D. Acosta *et al.* (CDF Collaboration), Phys. Rev. D **71**, 032001 (2005).

[11] V. M. Abazov *et al.* (DØ Collaboration), Phys. Rev. Lett. **94**, 161801 (2005).

[12] M. A. Aivazis, J. C. Collins, F. I. Olness and W. K. Tung, Phys. Rev. D **50**, 3102 (1994); J. C. Collins, Phys. Rev. D **58**, 094002 (1998); J. Pumplin *et al.*, JHEP **0207**, 012 (2002).

[13] A. Aktas *et al.* (H1 Collaboration), Eur. Phys. J. C **45**, 23 (2006); A. Aktas et al., Eur. Phys. J. C **40**, 349 (2005).

[14] C. S. Hill *et al.*, Nucl. Instrum. Methods A **530**, 1 (2004).

[15] A. Sill *et al.*, Nucl. Instrum. Methods A **447**, 1 (2000).

[16] A. Affolder *et al.*, Nucl. Instrum. Methods A **453**, 84 (2000).

[17] A. Affolder *et al.*, Nucl. Instrum. Methods A **526**, 259 (2004).

[18] D. Acosta *et al.* (CDF Collaboration), Phys. Rev. D **71**, 032001 (2005).

[19] L. Balka *et al.*, Nucl. Instrum. Methods A **267**, 272 (1988).

[20] S. Bertolucci *et al.*, Nucl. Instrum. Methods A **267**, 301 (1988).

[21] M. Albrow *et al.*, Nucl. Instrum. Methods A **480**, 524 (2002).

[22] A. Bhatti *et al.*, arXiv:hep-ex/0510047, submitted to Nucl. Instrum. Methods.

[23] G. Ascoli *et al.*, Nucl. Instrum. Methods A **268**, 33 (1988).

[24] D. Acosta *et al.*, Nucl. Instrum. Methods A **461**, 540 (2001).

[25] T. Sjöstrand and S. Mrenna, LU-TP 01, arXiv:hep-ph/0108264.

[26] H.L. Lai *et al.*, Eur. Phys. J. C **12**, 375 (2000).

[27] D. Acosta *et al.* (CDF Collaboration), Phys. Rev. D **70**, 072002 (2004).

[28] P. Avery, H. Read and G. Trahern, CLEO Report CSN-212 (1985), unpublished.

[29] GEANT, Detector description and simulation tool, CERN Program Library Long Writeup W5013 (1993).

[30] E. Gerchtein and M. Paulini, Computing in High Energy and Nuclear Physics, preprint arXiv:physics-0306031, (2003).

[31] P. Sutton, A. D. Martin, R. Roberts and W. Stirling, Phys. Rev. D **45**, 2349 (1992); R. Rijken and W. van Neerven, Phys. Rev. D **51**, 44 (1995); R. Hamberg, W. van Neerven and T. Matsuura, Nucl. Phys. B **359**, 343 (1991); R. Harlander and W. Kilgore, Phys. Rev. Lett. **88**, 201801 (2002); W. van Neerven and E. Zijstra, Nucl. Phys. B **382**, 11 (1992).

[32] N. Kidonakis, R. Vogt, Eur. Phys. J. C **33**,466-S468 (2004).

[33] J. Campbell and R.K. Ellis, Phys. Rev. D **60**, 113006 (1999).

[34] F. Abe *et al.* (CDF Collaboration), Phys. Rev. Lett. **75**, 3997 (1995).

[35] D. Acosta *et al.* (CDF Collaboration), Phys. Rev. D **71**, 052003 (2005).

[36] D. J. Jackson, Nucl. Instrum. Methods A **388** (1997) 247. J. Abdallah *et al.* (DELPHI Collaboration), Eur. Phys. J. C **32** (2004) 185.

[37] M. D'Onofrio, Ph. D. thesis, University of Geneva (2006).

[38] R. Barlow and C. Beeston, Comp. Phys. Comm. **77** (1993) 219.

[39] G. Corcella *et al.*, JHEP **0101** (2001) 010.

[40] A. Abulencia *et al.* (CDF Collaboration), arXiv:hep-ex/0510048, submitted to Phys. Rev. D.

[41] LEP/SLD Heavy Flavour Working Group, D. Abbaneo *et al.*, LEPHF 2001-01; (available from http://lepewwg.web.cern.ch/LEPEWWG/heavy/).

[42] S. Klimenko, J. Konigsberg, and T.M. Liss, FERMILAB-FN-0741 (2003).

[43] private communication from J. Campbell.

[44] J. Pumplin *et al.*, JHEP **07**, 012 (2002).